F-3-2

Extended Abstracts of the 2014 International Conference on Solid State Devices and Materials, Tsukuba, 2014, pp688-689

Development of Ferroelectric Phase in TiN/Hf-Zr-O/TiN Capacitors Prepared by Sputter Deposition and Capped Anneal

Shinji Migita, Hiroyuki Ota, Yukinori Morita, and Meishoku Masahara

Nanoelectronics Research Institute
National Institute of Advanced Industrial Science and Technology (AIST)
West 7, Onogawa16-1, Tsukuba, Ibaraki 305-8569, Japan
E-mail: s-migita@aist.go.jp

Abstract

Electrical properties of Hf-Zr-O films are examined in metal-insulator-metal capacitors. It is found that capped anneal process promotes transition of crystalline phases and induces ferroelectric behavior at 50/50 ratio of Hf/Zr composition. Correlation of ferroelectricity with the Hf/Zr composition and the film thickness are systematically investigated.

1. Introduction

Ferroelectric materials are attractive in a wide range of electronic applications such as piezo-electric, memory, and logic devices. Recently, existence of ferroelectric property in a metastable HfO_2 system was reported and widely investigated [1-6]. It is demonstrated by doping of Si, Y, Sr, Ga, and La in HfO_2 films, and forming compound films of $Hf_{0.5}Zr_{0.5}O_2$. In all cases, ferroelectric property is closely correlated with the chemical composition and annealing conditions. One of the key processes is the capped-annealing (Cap-PDA) [7]. This process promotes formation of metastable crystalline phases in HfO_2 systems, and contributes to the enhancement of dielectric constant.

In this work, we examined the reproducibility of ferroelectricity in Hf-Zr-O system, and investigated the dependence on chemical composition and film thickness.

2. Experimental

Metal-insulator-metal (MIM) capacitors, consist of TiN bottom electrode, Hf-Zr-O dielectric films, and TiN top electrodes, were fabricated (**Fig. 1**). Crystallization of Hf-Zr-O films was processed by the Cap-PDA technique. In order to control the chemical composition of Hf-Zr-O films, a sputtering system that equips multiple *RF* sputtering sources with a time-sharing of shuttering time (**Fig. 2**). Chemical compositions and deposition rates were confirmed by x-ray photoelectron spectroscopy and ellipsometry (**Fig. 3**). C-V and I-V characteristics were measured using the LCR meter (Agilent 4284A) and the semiconductor parameter analyzer (Agilent 4156C) at room temperature.

3. Results and Discussion

The impact of Cap-PDA on the crystalline phases of $Hf_{0.5}Zr_{0.5}O_2$ films is analyzed by in-plane XRD (**Fig. 4**). In case of the analysis of Cap-PDA sample, the top TiN film was removed beforehand by dry etching. A monoclinic phase crystal film is formed by the conventional PDA. In contrast, Cap-PDA changes the crystalline phase drastically, although it is hard to distinguish the phase between cubic, tetragonal, and orthorhombic. Formation of the ferroelectric film is confirmed by the hysteretic loop in the C-V measurement (**Fig. 5**). However, it is interesting that a sign of ferroelectricity is observable even in the PDA sample. It suggests that the bottom TiN electrode is also responsible for the formation of metastable phase although the volume fraction is small. Leakage current levels are the same irrespective of annealing processes.

The influence of Hf/Zr composition on electrical properties is examined (**Fig. 6**). Film thickness is unified to 10 nm, and processed by Cap-PDA. Ferroelectric loop appears only in a restricted chemistry range, 50/50 to 40/60 ratio of Hf/Zr composition. This is reasonable with the preceding report [2]. It is noted that both C-V and I-V curves in all cases are asymmetric against the polarity of bias voltage. The properties of Hf-Zr-O interfaces between top and bottom electrodes might be dissimilar.

Thickness dependences of C-V characteristics in $Hf_{0.5}Zr_{0.5}O_2$ films are plotted (**Fig. 7**). Ferroelectric hysteresis loop is distinguished between 8.0 nm and 10.6 nm. For the thinnest case, 5.3 nm film, verification of ferroelectricity was disturbed by the large leakage current. For the thick film cases in contrast, although the leakage current is well suppressed, ferroelectric property decayed with the increment of thickness.

Effects of chemical composition and film thickness on physical properties are summarized (**Fig. 8**). The dielectric constant ε_r was chosen at the value of 0 V, and the ferroelectric charge Q_F was calculated by the integration of hysteresis loop in the C-V curve and averaged between the positive and negative bias region. Emergence of ferroelectric property is correlated with the enhancement of the dielectric constant in Fig. 8(a). It implies that the ferroelectric phase is a product around the morphotropic phase boundary (MPB). In addition, thickness dependence in Fig. 8(b) brings a question about the driving force of phase transition. Similar trend was reported in the formation of higher-k HfO_2 MIS capacitors through Cap-PDA [8]. It is probable that the phase transition is driven by mechanical stress and/or oxygen absorption by metal electrodes. Although it is hard to distinguish these effects, it is common that interface between Hf-Zr-O and metal electrode has a crucial role.

4. Conclusions

Ferroelectric behavior of Hf-Zr-O system is successfully reproduced in MIM structures. The sensitivity with the chemical composition suggests that it is induced by the nature at MPB. Dependence of film thickness infers that it is driven at the interface between Hf-Zr-O film and metal electrode.

Acknowledgements

The research is partly granted by JSPS through the First Program initiated by CSTP.

References

[1] T. S. Böscke *et al.*, Appl. Phys. Lett. **99**, 102903 (2011); Appl. Phys. Lett. **99**, 112904 (2011). IEDM 2011, p. 547;
[2] J. Müller *et al.*, Appl. Phys. Lett. **99**, 112901 (2011); J. Appl. Phys. 110, 114113 (2011); Nano Lett. **12**, 4318 (2012); IEEE EDL 33, 185 (2012); VLSI 2012 p. 25; IEDM 2013, p. 280.
[3] D. Zhou *et al.*, Appl. Phys. Lett. **100**, 082905 (2012).
[4] S. Müller *et al.*, IEEE EDL **33**, 1300 (2012).
[5] T. Olsen *et al.*, Appl. Phys. Lett. **101**, 082905 (2012).
[6] M. H. Park *et al.*, Appl. Phys. Lett. **102**, 242905 (2013).
[7] S. Migita *et al.,* VLSI Tech. 2008, p. 152.
[8] Y. Morita et al., Jpn. J. Appl. Phys. **41**, 02BA04 (2012).

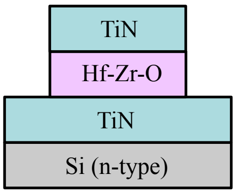

1. Si substrate: HF cleaning
2. TiN deposition (40 nm)
3. Hf-Zr-O deposition
4. TiN deposition (40 nm)
5. Cap-PDA (600°C, 20 s)
6. Patterning by dry etching

Fig. 1. Schematic diagram of MIM capacitor ($1\text{x}10^{-4}$ cm^2) fabricated in this work and typical process conditions.

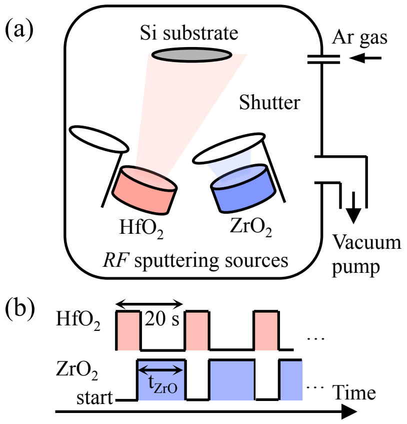

Fig. 2. (a) Deposition system for Hf-Zr-O compound films. (b) Sequence of opening and shuttering for the control of chemical composition.

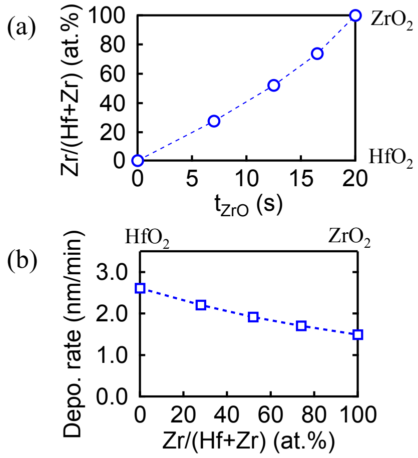

Fig. 3. (a) Chemical composition of Hf-Zr-O films with ZrO_2 supply time. (b) Deposition rate of Hf-Zr-O films.

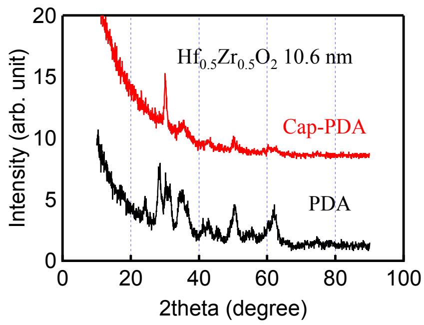

Fig. 4. In-plane XRD analysis of $Hf_{0.5}Zr_{0.5}O_2$ films (10.6 nm) prepared by Cap-PDA and PDA.

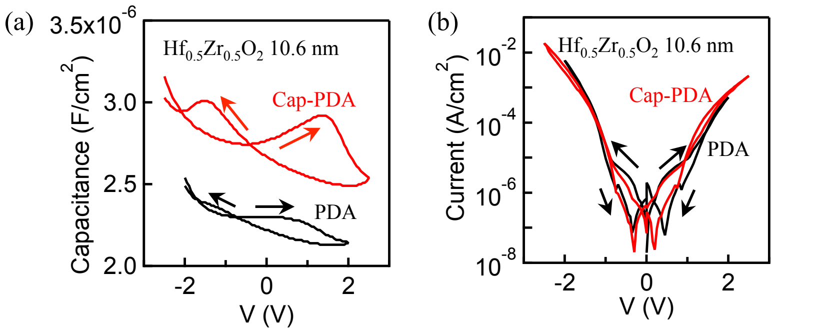

Fig. 5. (a) C-V and (b) I-V characteristics of $Hf_{0.5}Zr_{0.5}O_2$ films (10.6 nm) prepared by Cap-PDA and PDA.

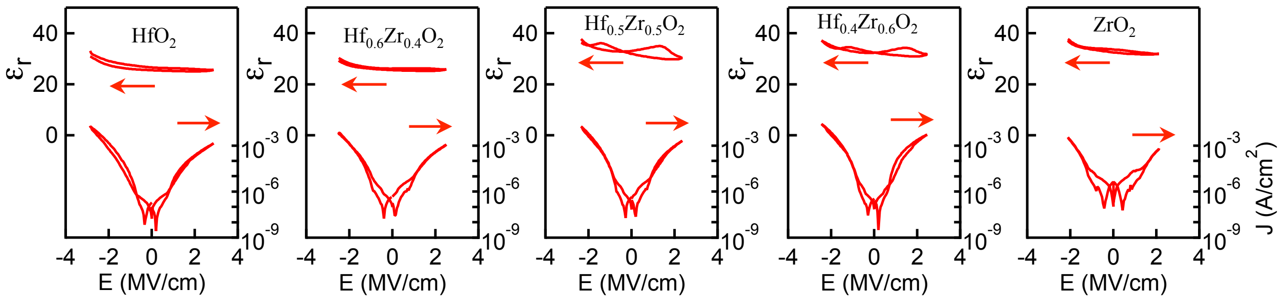

Fig. 6. εr-E and J-E characteristics of Hf-Zr-O capacitors (10 nm) prepared by Cap-PDA.

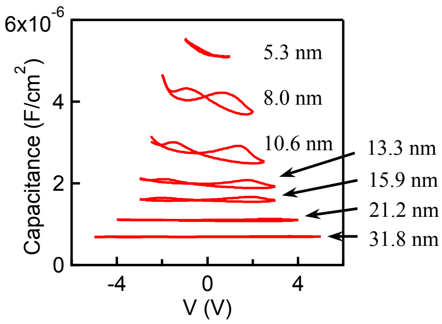

Fig. 7. Thickness dependence of C-V characteristics of $Hf_{0.5}Zr_{0.5}O_2$ capacitors prepared by Cap-PDA.

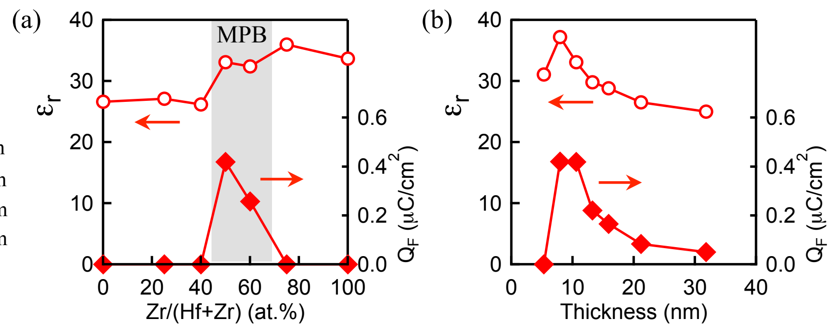

Fig. 8. Dependences of dielectric constant (εr) and ferroelectric charge (Q_F) on (a) chemical composition of Hf-Zr-O films (10 nm) and (b) thickness of $Hf_{0.5}Zr_{0.5}O_2$ films, prepared by Cap-PDA (600°C, 20s).